

# Air/Water Path Switching with Beam Steering for Water Distance/Turbidity Adaptive Underwater Optical Wireless Communication Network: Concept and Demonstration

Kiichiro Kuwahara<sup>1</sup>, Hyuga Nagami<sup>1</sup>, Keita Tanaka<sup>1</sup>, Fumiya Kobori<sup>1</sup>, Ayumu Kariya<sup>1</sup>, Shogo Hayashida<sup>2</sup>,  
and Takahiro Kodama<sup>1</sup>

<sup>1</sup>Faculty of Engineering, Kagawa University 2217-20 Hayashi-machi, Takamatsu-shi, Kagawa, 761-0396 Japan

<sup>2</sup>LED Backhaul Project, Sangikyo Corporation, 4509 Ikebe-machi, Tsuzuki-ku, Yokohama-shi, Kanagawa, 224-0053 Japan  
[kodama.takahiro@kagawa-u.ac.jp](mailto:kodama.takahiro@kagawa-u.ac.jp)

**Abstract:** We conducted full-duplex class 1 eye-safe transmission experiments, including 4K video demonstrating robust connectivity to maximize transmission capacity under optimal paths by introducing aerial relay nodes within underwater optical wireless communication networks in shallow seas. (tel: +81 87.864.2231, e-mail: [kodama.takahiro@kagawa-u.ac.jp](mailto:kodama.takahiro@kagawa-u.ac.jp)). © 2024 The Author(s)

## 1. Introduction

In the context of the next-generation mobile communication standard, 6G, there is a growing anticipation for the deployment of optical wireless communication (OWC) systems in non-terrestrial networks [1–3]. Beam steering is an important technology for realizing highly accurate OWC systems [4]. One of the notable applications within this domain is the underwater OWC system in shallow marine areas, which experiences substantial variations in received signal power due to shifts in turbidity and transmission distance [5]. Consequently, employing adaptive modulation schemes to maximize transmission capacity, based on the received signal-to-noise ratio (SNR), proves highly effective. In underwater OWC systems, visible light in the 450 nm to 550 nm range is preferred for long-distance transmission, primarily due to minimal losses in the underwater channel [6]. Additionally, the use of non-visible light spectrum is desirable for enhanced confidentiality in the vicinity of human habitation in shallow waters. A previous study investigated the use of 850 nm infrared light-based frequency-domain adaptive modulation signals in underwater communication channels [7]. However, situations where adaptive modulation cannot adequately adapt to changes in transmission distance and turbidity can lead to communication impairments, even when employing the lowest-order modulation schemes.

Simulated principle experimental demonstrations of air-water OWC system have been recently conducted, focusing on communication between underwater and aerial drones [8]. Utilizing air channels with relatively lower disturbances presents an approach that offers robustness against variations in underwater channel conditions. This approach holds greater promise than networks solely relying on underwater channels.

In this paper, we propose an optical network that seamlessly switches between air and water optical paths to maximize transmission capacity based on the transmission distance and turbidity of the underwater channel. The deployment of relay nodes equipped with large acrylic mirrors in the air enables the establishment of aerial optical paths by dynamically adjusting the beam angle from the optical transceiver and the light-receiving surface of the optical receiver. Through adaptive modulation and air/water optical path switching, we verified the practicality of this approach for facilitating 4K video transmission in full-duplex class 1 eye-safe underwater OWC systems, while adapting to changes in underwater turbidity and transmission distance. Furthermore, this paper introduces the concept of an underwater optical network that incorporates an aerial optical path by deploying aerial relay nodes; this novel report encompasses the interaction of two transceivers located within a shallow marine area.

## 2. Concept of air/water optical path switching network

Fig. 1 illustrates the configuration of a full-duplex underwater OWC system capable of switching between air and water optical paths. This method assumes that the spacing between two underwater transceivers varies as two underwater mobile terminals move. An aerial mobile relay node, positioned between the two underwater mobile terminals and controlled from the sea surface, adjusts its vertical position accordingly. The water optical path is selected when the transmission distance in the underwater channel is short or when the turbidity is low, resulting in a high received SNR. During water optical path selection, the two underwater transceivers engage in bidirectional beam transmission while facing each other. Conversely, the aerial optical path is chosen when the transmission distance in the underwater channel is extended or when turbidity is high, leading to a low received SNR. During aerial optical path selection, the two underwater transceivers transmit beams toward a mirror on the aerial node. The

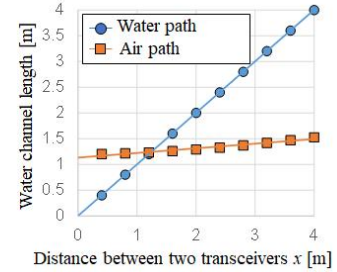
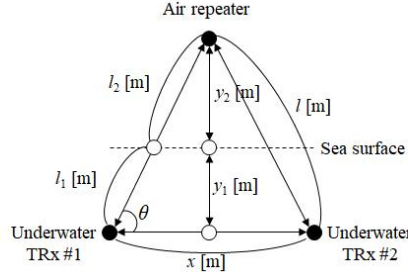
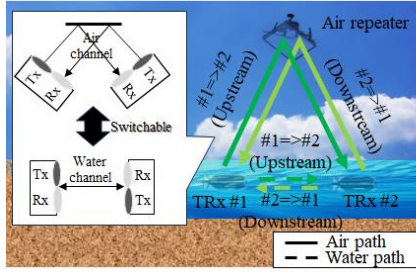


Fig. 1. Concept of air/water optical path switching. Fig. 2. Geometric element placement. Fig. 3. Water channel distance in air/water path.

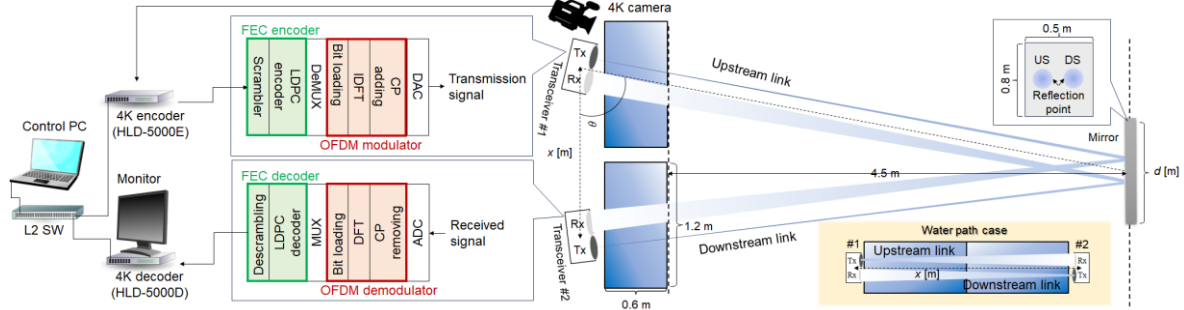


Fig. 4. Experimental setup of air/water optical pass switching.

angles of incidence and reflection are adjusted to match the mirror's orientation. Communication from transceiver #1 to #2 is referred to as upstream, while that in the reverse direction is termed downstream.

Fig. 2 depicts a geometric configuration diagram of the equipment. The distances between the underwater transceivers, the water depth at the underwater transceiver positions, and the height of the aerial relay node above the water surface is denoted as  $x$ ,  $y_1$ , and  $y_2$ , respectively. The distance from the underwater transceivers to the sea surface, that from the sea surface to the aerial relay node, and the total distance are denoted as  $l_1$ ,  $l_2$ , and  $l$ , respectively. Fig. 3 illustrates the underwater channel distances for both the air and water optical paths under the conditions of  $y_1 = 0.6$  m and  $y_2 = 0.45$  m while varying the parameter  $x$ . In the water optical path,  $x$  corresponds to the underwater channel distance. By contrast, in the aerial optical path, when  $x$  is small, underwater channel transmission is necessary; however, as  $x$  increases, the increase in underwater channel distance is relatively small. The boundary at which the relationship between air and water optical path distances changes is  $x = 1.2$  m.

### 3. Setup of proof-of-principle experiment

Fig. 4 illustrates an experimental setup for 4K video data transmission in a full-duplex eye-safe OWC system emulating air/water optical path switching. Both upstream and downstream processes were performed similarly, as described below. In the transmitter-side forward error correction (FEC) encoding section, the original data were processed through scrambling and low-density parity-check (LDPC) code encoding to generate a bit sequence with error correction codes added. The bit sequence was converted into symbols for each subcarrier using DeMUX. The selected modulation symbols were part of the  $M$ -value signals of quadrature amplitude modulation. In the OFDM signal modulation section, dynamic bit loading allocated bits to each subcarrier based on SNR. Subcarriers were generated using inverse discrete Fourier transform, and a guard interval was added using a cyclic prefix (CP) to improve resistance to symbol interference.

The OFDM signal with subcarrier multiplexing was output as an analog signal through a digital-to-analog converter. The 850 nm light emitted from the LED passed through the air and underwater channels inside the water tank. For the water optical path, the transmission distance of the underwater channel was varied by changing the orientation and the number of passages through the water tank. For the air optical path, the direction of the water tank and the position of the mirror were fixed, and the transmission distance of the air and water channels was changed by varying the transceiver spacing  $x$  and the incident angle  $\pi/2 - \theta$  to the mirror. The tank was filled with tap water or seawater with a turbidity of 2.2 nephelometric turbidity units. A photodiode converted the optical signal into an electrical signal at the receiver side. An analog-to-digital converter converted the electrical signal into a digital signal. In the OFDM signal demodulation section, subcarriers were separated using a discrete Fourier transform after removing the CP. Symbols for each subcarrier were converted into bit sequences using MUX. The original data were restored through LDPC decoding and descrambling in the FEC decoding section. This bit rate

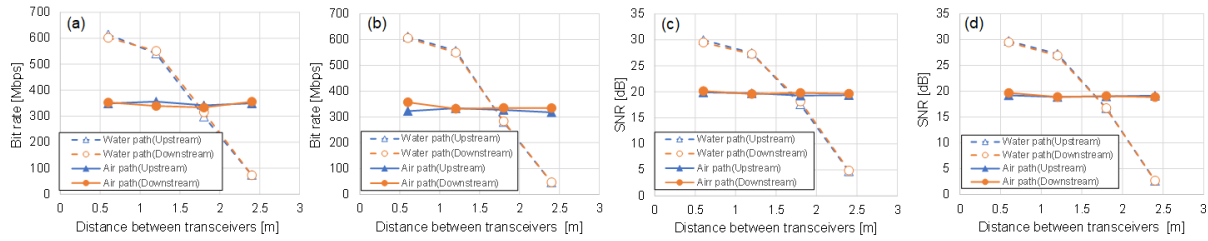


Fig. 5. Experimental results: (a) bit rate characteristics under tap water channel, (b) bit rate characteristics under shallow sea water channel, (c) SNR characteristics under tap water channel, and (d) SNR characteristics under shallow sea water channel.

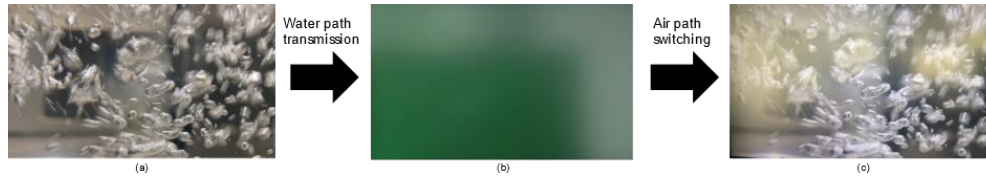


Fig. 6. 4K video data image (a) before transmission, for (b) water path channel at  $x = 2.4$  m, and for (c) air path channel at  $x = 2.4$  m.

evaluation's maximum transmission capacity for the distance between transceivers ensured error-correctable signal quality through adaptive modulation.

#### 4. Experimental results

In Figs. 5(a-d), we present the static characteristics of transmission distance versus SNR and transmission capacity, obtained under optimal optical transceiver configurations for both uplink and downlink in air/water optical paths. We evaluated the transmission using two types of water: tap water and shallow seawater. In the case of water optical paths, for both uplink and downlink, SNR and transmission capacity evidently exhibited exponential decay with variations in the transceiver spacing. Conversely, in the case of air optical paths, SNR and transmission distance remained nearly unaffected by changes in transceiver spacing. Notably, transitioning from water to air optical paths at a transceiver spacing of 1.8 m yielded superior characteristics. Figs. 6(a-c) illustrate the original data from a 4K video captured by a camera, along with images of the water optical path at  $x = 2.4$  m and the air optical path at  $x = 2.4$  m, respectively. Switching from a water optical path, where video transmission was not feasible, to an air optical path facilitated the delivery of 4K video content.

#### 5. Conclusions

We proposed a novel network designed for use in shallow water environments, allowing for the switching of air and water optical paths, and experimentally verified the network. The experiment demonstrated the feasibility of robust system operation without significant reduction in transmission capacity by switching between air and water optical paths, with the boundary defined at a distance of 1.9 m from the optical transceivers placed at a water depth of 0.6 m.

*We would like to thank to Mr. A. Iwata and R. Komatsubara of IBEX Technology, Mr. T. Matsui, and Mr. S. Yamamoto, and Mr. T. Suda of Sangikyo Corporation for their cooperation in carrying out the experiments conducted for this research.*

#### References

- [1] C.W. Chow, C. H. Yeh, Y. Liu, Y. Lai, L. Y. Wei, C. W. Hsu, G. H. Chen, X. L. Liao, and K. H. Lin, "Enabling technologies for optical wireless communication systems," *Proc. Optical Fiber Communication Conference (OFC)*, M2F.1, Mar. 2020.
- [2] K. Wang, T. Song, Y. Wang, C. Fang, J. He, A. Nirmalathas, C. Lim, E. Wong, and S. Kandeepan, "Evolution of short-range wireless communications," *IEEE Journal of Lightwave Technology*, vol. 41, no. 4, pp. 1019-1040, Feb. 2023.
- [3] Z. Hu, Z. Chen, Y. Li, D. M. Benton, A. A. I. Ali, M. Patel, M. P. J. Lavery, and A. D. Ellis, "Adaptive transceiver design for high-capacity multi-modal free-space optical communications with commercial devices and atmospheric turbulence," *IEEE Journal of Lightwave Technology*, vol. 41, no. 11, pp. 3397-3406, June 2023.
- [4] A. Derakhshandeh, S. Pachnicke, and P. A. Hoeher, "Underwater wireless laser-based communications using optical phased array antennas," *IEEE Photonics Journal*, vol. 15, no. 5, pp. 1-9, Oct. 2023.
- [5] P. A. Hoeher, J. Sticklus, and A. Harlakin, "Underwater optical wireless communications in swarm robotics: A tutorial," *IEEE Communications Surveys & Tutorials*, vol. 23, no. 4, pp. 2630-2659, Fourthquarter 2021.
- [6] H. Kaushal and G. Kaddoum, "Underwater optical wireless communication," *IEEE Access*, vol. 4, pp. 1518-1547, 2016.
- [7] A. Kariya, K. Tanaka, F. Kobori, T. Ishikawa, S. Hayashida, and T. Kodama, "Completely invisible underwater wireless optical communication system: full-duplex transmission in 1.9 m shallow-water channel with 3m/s wind," *Proc. Optoelectronics Global Conference (OGC 2023)*, 1804, Shenzhen, China, Sept. 2023.
- [8] K. Tanaka, A. Kariya, F. Kobori, K. Shimada, S. Hayashida, and T. Kodama, "Demonstration of full-duplex and real-time transmission over 10 m Air and 1.2 m water channel for completely invisible optical wireless communication systems," *Proc. Photonic Networks and Devices (Networks)*, NeW4B.2, Busan, July 2023.